

Fast Density Estimation for Density-based Clustering Methods

Difei Cheng, *Student Member, IEEE*, Ruihang Xu, *Student Member, IEEE*, Bo Zhang, *Member, IEEE*, and Ruinan Jin, *Student Member, IEEE*,

Abstract—Density-based clustering algorithms are widely used for discovering clusters in pattern recognition and machine learning. They can deal with non-hyperspherical clusters and are robust to outliers. However, the runtime of density-based algorithms is heavily dominated by neighborhood finding and density estimation which is time-consuming. Meanwhile, the traditional acceleration methods using indexing techniques such as KD trees may not be effective in dealing with high-dimensional data. To address these issues, this paper proposes a fast range query algorithm, called Fast Principal Component Analysis Pruning (FPCAP), with the help of the fast principal component analysis technique in conjunction with geometric information provided by the principal attributes of the data. FPCAP can deal with high-dimensional data and can be easily applied to density-based methods to prune unnecessary distance calculations in neighborhood finding and density estimation. As an application in density-based clustering methods, FPCAP is combined with the Density Based Spatial Clustering of Applications with Noise (DBSCAN) algorithm, and an improved DBSCAN (called IDBSCAN) is then obtained. IDBSCAN preserves the advantage of DBSCAN and, meanwhile, greatly reduces the computation of redundant distances. Experiments on seven benchmark datasets demonstrate that the proposed algorithm improves the computational efficiency significantly.

Index Terms—Density-based Clustering, Principle component analysis, Pruning.

I. INTRODUCTION

CLUSTERING aims to partition a set of data objects into several clusters so that objects in each cluster keep high degree of similarity, and thus has been widely used in data mining [1], vector quantization [2], dimension reduction [3] and manifold learning [4].

Density-based clustering is one of the most important clustering methods. It is based on density estimation of data points and defines clusters as dense regions separated by low-density regions. It does not need to know the number of clusters, and meanwhile, it has the ability to discover clusters with arbitrary shapes and is robust to outliers. So far, many density-based methods have been proposed, such as DBSCAN [5], the Ordering Points To Identify the Clustering Structure (OPTICS) [6], Clustering by Fast Search and Find of Density Peaks (CFSFDP) [7] and Mean-Shift Clustering [8], [9].

D. cheng, R. Xu and R. Jin are with Academy of Mathematics and Systems Science, Chinese Academy of Sciences, Beijing 10090, China and School of Mathematical Sciences, University of Chinese Academy of Sciences, Beijing 10049, China

B. Zhang is with LSEC and Academy of Mathematics and Systems Science, Chinese Academy of Sciences, Beijing 100190, China and School of Mathematical Sciences, University of Chinese Academy of Sciences, Beijing 100049, China (email: b.zhang@amt.ac.cn) **Corresponding author: Bo Zhang**

DBSCAN is probably the most prominent density-based clustering algorithm so far. It is based on the key idea that for each core data point of a cluster its neighborhood of a given radius ϵ has to contain at least a minimum number of data points (MinPts). However, DBSCAN has some disadvantages. First, the parameters ϵ and MinPts have a significant influence on the clustering results and are difficult to choose. OPTICS [6] was then proposed to overcome this difficulty by creating an augmented ordering of the database representing a density-based clustering structure which includes the information of the clustering results obtained by DBSCAN corresponding to a broad range of parameters settings. Secondly, the time complexity of DBSCAN is $O(n^2)$. Thus many improved methods have been proposed to accelerate DBSCAN, which can be roughly divided into two categories: sampling-based improvements and partition-based improvements. Sampling-based methods [10]–[14] try to reduce the number of range queries by skipping some queries from specific points in the process of finding neighbors and calculating the density of each point, whilst partition-based methods [15]–[17] use grid partitions to divide the data into several groups to process separately. When finding neighbors, most of the above improved DBSCAN algorithms speed up DBSCAN by reducing the number of range queries. But some sampling-based methods, such as those in [10] and [14], still need to calculate the $\epsilon/2$ -neighborhoods and 2ϵ -neighborhoods many times. Thus it is important to reduce the range query time during neighborhood finding. Traditionally, indexing techniques such as KD-tree [18], Cover tree [19], quadtree-like hierarchical tree [19] and R tree [20] are used to reduce the range query time in these sampling-based algorithms. However, the construction of the tree structures is complex, and these indexing techniques such as KD tree are very difficult to deal with high-dimensional data sets.

Motivated by the work in [21] which applies the Fast Principal Component Analysis (Fast-PCA) technique [22] in accelerating the global k -means algorithm [23], we propose a fast range queries method (called FPCAP), based on the Fast-PCA technique in conjunction with certain geometric information provided by the principal attributes of the data. FPCAP can greatly reduce the range query time by reducing the computation of redundant distances during neighborhood finding and density estimation, and meanwhile, it avoids any complex data structures which are needed to embed the data points themselves and are not easy to implement. Further, FPCAP can deal with high-dimensional data sets. In experiments, FPCAP is compared with the KD tree indexing technique. As

an application in density-based clustering methods, FPCAP is applied to DBSCAN to obtain an improved DBSCAN algorithm which is called IDBSCAN. IDBSCAN is compared with the original DBSCAN algorithm as well as the original DBSCAN algorithm with the KD tree indexing technique. The experimental results on seven clustering benchmark datasets illustrate that both FPCAP and IDBSCAN outperform the other compared algorithms on computational efficiency. In addition, IDBSCAN is an exact DBSCAN algorithm which produces the same results as did by DBSCAN.

The remaining part of the paper is organized as follows. In Section II, we briefly introduce some related work, the DBSCAN algorithm, the Fast-PCA algorithm and the KD-tree algorithm. Our proposed algorithm is proposed in Section III. Experimental results are provided in Section IV, and conclusions are given in Section V.

II. RELATED WORK

A. The DBSCAN algorithm

DBSCAN [5] has two important parameters ε and MinPts. A point x is called a core point if the number of points within the ε -neighborhood of x is more than MinPts. A point y is called directly density-reachable from a core point x if y is in the ε -neighborhood of x . A point y is called density-reachable from a core point x if there is a series of points y_1, y_2, \dots, y_n with $y = y_n, x = y_1$ and for any pair y_i, y_{i+1} we have that y_{i+1} is directly density-reachable from y_i . Two points are density-connected if they both are density-reachable from the same core point. A cluster C in DBSCAN satisfies the following two conditions:

- Maximality: any point which is density-reachable from a core point in cluster C is also in cluster C .
- Connectivity: any two points in cluster C are density-connected.

Details of DBSCAN are described in Algorithm 1.

B. Fast-PCA

Fast-PCA [22] is designed to find h leading eigenvectors by using a fixed-point algorithm [24]. Its computational cost is much less than that of the eigenvalue decomposition (EVD) based PCA. Algorithm 2 presents details of Fast-PCA.

C. KD-tree

KD-tree was introduced by Bentley [18], [25] as a binary tree that stores k -dimensional data. As a famous space-partitioning data structure used to organize points in a k -dimensional space, KD-tree subdivides data like a binary tree at each recursive level of the tree but uses k keys for all levels of the tree which is different from a binary tree that uses a single key. For example, to build a KD-tree from three-dimensional points in the (x, y, z) coordinates, the coordinate of keys would be chose circularly from x, y, z for successive levels of the KD-tree. A often-used scheme for cycling the keys chooses the coordinate that has the widest dispersion or largest variance to be the key for a particular level of recursion, and the splitting node is positioned at the spatial median of the

Algorithm 1 The DBSCAN algorithm

Input: $D = \{x_1, x_2, \dots, x_n\}$, ε , MinPts

Output: *classifications*

- 1: Initialize *classifications* to an n -dimensional vector with its component being Unclassified; $seed = \emptyset$; $cluster_id = 1$; $ID = 1$; $id = 1$
- 2: Calculate $N_\varepsilon(x_{id}) = \{x \in D | d(x, x_{id}) < \varepsilon\}$, where $x_{id} \in D$ and $d(x, y)$ denotes the distance between two points.
- 3: If $|N_\varepsilon(x_{id})| < \text{MinPts}$ and x_{id} 's classification is Unclassified, then *classifications*(id) is Noise, where $|D|$ denotes the cardinality of the set D ; otherwise, for every point y whose classification is Unclassified or Noise in $N_\varepsilon(x_{id})$, we set

$$classifications(p) := cluster_id,$$

where p is index of y , and if y 's classification is Unclassified, update $seed = seed \cup \{y\}$.

- 4: If $seed \neq \emptyset$, update $seed = seed/x_{id}$
 - 5: If $seed \neq \emptyset$, choose a point y in $seed$, update $id = index\ of\ y$ and go back to Step 2. Otherwise, if *classification*(id) = $cluster_id$, update $cluster_id = cluster_id + 1$
 - 6: Update $ID = ID + 1$, $id = ID$. If *classifications*(id) is Unclassified, go back to Step 2; otherwise, go back to Step 6 until $ID = n$.
-

Algorithm 2 Fast-PCA

Input: Data $X = [X_1, \dots, X_h]$ of size $n \times h$, where X_i is the i th feature with size $n \times 1$ and $\sum X_i = 0$, that is, X is assumed to be zero-centered, and the desired number h of leading eigenvectors.

Output: projection of data, Z , with size $n \times h$.

- 1: Compute covariance $\sum_X = XX^T$, and set $p = 1$
- 2: Randomly initialize eigenvector ϕ_p of size $n \times 1$
- 3: Update ϕ_p as $\phi_p \leftarrow \sum_X \phi_p$
- 4: Do the Gram-Schmidt orthogonalization process for ϕ_p :

$$\phi_p \leftarrow \phi_p - \sum_{j=1}^{p-1} (\phi_p^T \phi_j) \phi_j \quad (1)$$

- 5: Normalize ϕ_p by dividing it by its norm:

$$\phi_p \leftarrow \phi_p / \|\phi_p\| \quad (2)$$

- 6: If ϕ_p has not converged, go back to Step 3. (The Fast-PCA algorithm for the p -th basis vector converges when the new and old values ϕ_p point in the same direction, i.e. $(\phi_p^+)^T \phi_p \approx 1$, where ϕ_p^+ is the new value of ϕ_p).
 - 7: Set $p = p + 1$ and go to Step 2 until $p = h$
 - 8: Get the orthogonal projection matrix: $\Phi = [\phi_1, \phi_2, \dots, \phi_h]$. The columns of the projection matrix are sorted by the descending order of the corresponding eigenvalues.
 - 9: Get the projection of data: $Z = X\Phi$
-

chose coordinate. As an acceleration structure, it has been used in a variety of applications, including range queries for fixed-radius near neighbors and nearest neighbors searching. For example, the KD-tree indexing technique is frequently used for the range query in the process of finding fixed-radius near neighbors or calculating densities in density-based clustering. When the KD-tree is used for range queries, it first locates the smallest sample subspace according to the judgment method of a binary tree and then backtracks each parent node. When the distance between the target point and the parent node is less than the threshold, the searching enters another subspace of the parent node.

III. THE PROPOSED ALGORITHM

A. Fast-PCA pruning

For a given data set D of n points, it is time-consuming to find neighbors for each point by simply comparing the distances between the point and all other $n - 1$ points in the data set, which has a time complexity of $O(n^2h)$, where h is the dimension of the data. An indexing technique can be used to accelerate the above process of finding neighbors, but it is difficult to deal with high-dimensional data. To address this issue, we propose a fast range query algorithm to reduce the redundant distance calculations and improve the computational efficiency, based on Fast-PCA in conjunction with some geometric information provided by the principal attributes of the data.

Let $D = \{x_1, x_2, \dots, x_n\}$ be a set of data points, where x_i is an h -dimensional vector and can be represented as $x_i = \sum_{j=1}^h x_{i,j} e_j$ with the e_j 's being the h -dimensional orthonormal basis vectors. Take $X = [x_1^T, x_2^T, \dots, x_n^T]$ in Algorithm 2 and denote by ϕ_i the eigenvector corresponding to the i th largest eigenvalue, $i = 1, \dots, h$, obtained by Algorithm 2. Then x_i can be rewritten as $x_i = \sum_{j=1}^h z_{i,j} \phi_j$, where $z_{i,j} = \langle x_i, \phi_j \rangle$. In fact, $Z = (z_{i,j})_{n \times h}$ which is the projection of data obtained by Algorithm 2. For any $x_i \in D$ define

$$x_i := \hat{z}_i + \tilde{z}_i, \quad (3)$$

where $\hat{z}_i = \sum_{j=1}^{h_1} z_{i,j} \phi_j$, $\tilde{z}_i = \sum_{j=h_1+1}^h z_{i,j} \phi_j$ and h_1 is an integer which is less than h and to be determined later. Then

$$\begin{aligned} \|x_i - x_j\|^2 &= \langle x_i - x_j, x_i - x_j \rangle \\ &= \langle (\hat{z}_i + \tilde{z}_i) - (\hat{z}_j + \tilde{z}_j), (\hat{z}_i + \tilde{z}_i) - (\hat{z}_j + \tilde{z}_j) \rangle \\ &= \langle \hat{z}_i - \hat{z}_j, \hat{z}_i - \hat{z}_j \rangle + \langle \tilde{z}_i - \tilde{z}_j, \tilde{z}_i - \tilde{z}_j \rangle \\ &= \|\hat{z}_i - \hat{z}_j\|^2 + \|\tilde{z}_i - \tilde{z}_j\|^2 \\ &\geq \|\hat{z}_i - \hat{z}_j\|^2 + \|\tilde{z}_i\| - \|\tilde{z}_j\|^2, \end{aligned} \quad (4)$$

where the Cauchy-Schwarz inequality is used to obtain the last inequality. The following results follow easily from (4).

Theorem 1. Given two points $x_i, x_j \in D$ with the form (3),

(i) if $\|\hat{z}_i - \hat{z}_j\| > \varepsilon$ then $x_i \notin N_\varepsilon(x_j)$, where $N_\varepsilon(x_j)$ is an ε -neighborhood of x_j ;

(ii) if $\|\hat{z}_i - \hat{z}_j\|^2 + \|\tilde{z}_i\| - \|\tilde{z}_j\|^2 > \varepsilon^2$ then $x_i \notin N_\varepsilon(x_j)$.

By Theorem 1 (i), if $\|\hat{z}_i - \hat{z}_j\| > \varepsilon$ then it is known that x_i is not in the ε -neighborhood of x_j without calculating

the distance between x_i and x_j . The time complexity of calculating the distance $\|x_i - x_j\|$ for each pair of points $x_i, x_j \in D$ is $O(n^2h)$, whilst that of calculating $\|\hat{z}_i - \hat{z}_j\|$ is $O(n^2h_1)$ for each pair of points \hat{z}_i, \hat{z}_j corresponding to the points $x_i, x_j \in D$. Since \hat{z}_i and \hat{z}_j are the projections of x_i and x_j on the space spanned by the eigenvectors $\phi_1, \dots, \phi_{h_1}$ corresponding to the largest h_1 eigenvalues and h_1 is usually much smaller than h , the calculation of $\|\hat{z}_i - \hat{z}_j\|$ is faster than that of $\|x_i - x_j\|$. In fact, the value of h_1 can be determined to be the smallest number of d such that the following inequality is satisfied for a given real number p :

$$\frac{\sum_{i=1}^d \lambda_i}{\sum_{j=1}^h \lambda_j} \geq p, \quad (5)$$

where λ_i is the i th largest eigenvalue. In the experiments conducted in Section IV, p can be taken as 0.7, 0.8, 0.9 or 0.99, and in such cases, h_1 is smaller than $h/2$ for most of the data sets. This means that Theorem 1 (i) can be used to exclude the data points x_i 's that are not in the ε -neighborhood of x_j with a lower computational cost by only verifying whether or not $\|\hat{z}_i - \hat{z}_j\| > \varepsilon$ for their projections \hat{z}_i and \hat{z}_j on the space spanned by the eigenvectors $\phi_1, \dots, \phi_{h_1}$ corresponding to the largest h_1 eigenvalues.

On the other hand, in the case when $\|\hat{z}_i - \hat{z}_j\| < \varepsilon$, we do not know if x_i is still in the ε -neighborhood of x_j . However, this can be justified with Theorem 1 (ii) by further calculating $\|\tilde{z}_i\| - \|\tilde{z}_j\|^2$ with a much lower cost. In fact, since

$$\begin{aligned} \|\tilde{z}_i\|^2 &= \langle \tilde{z}_i, \tilde{z}_i \rangle = \langle x_i - \hat{z}_i, x_i - \hat{z}_i \rangle \\ &= \langle x_i, x_i \rangle + \langle \hat{z}_i, \hat{z}_i \rangle - 2\langle x_i, \hat{z}_i \rangle \\ &= \langle x_i, x_i \rangle - \langle \hat{z}_i, \hat{z}_i \rangle \\ &= \|x_i\|^2 - \|\hat{z}_i\|^2, \end{aligned}$$

we have

$$\|\tilde{z}_i\| = (\|x_i\|^2 - \|\hat{z}_i\|^2)^{1/2}. \quad (6)$$

This means that $\|\tilde{z}_i\| - \|\tilde{z}_j\|$ can be calculated with $O(nh)$ time-complexity. In fact, $\|\tilde{z}_i\| - \|\tilde{z}_j\|$ can be calculated and stored in advance.

By the discussions above it is known that Theorem 1 can be used to exclude the data points x_i 's that are not in the ε -neighborhood of x_j with the time complexity $O(n^2h_1) + O(nh)$ which is lower than $O(n^2h)$ since, in general, $h_1 \ll h$. However, if the conditions in Theorem 1 (i) and (ii) are not satisfied, then we need to calculate the distance between x_i and x_j to see if x_i is in the ε -neighborhood of x_j .

For a single-range query, Theorem 1 helps to reduce the time complexity in the neighborhood finding process from $O(n^2h)$ to $O(n^2h_1) + O(nh)$. This is a good improvement when $h = O(n)$ and $h_1 \ll h$. However, if n is large enough, the $O(n^2)$ time-complexity is still quite high, and so it is necessary to further reduce the time complexity by reducing the number of accesses during range query, that is, we use Theorem 1 to deal with only small part of the other $n - 1$ points in finding the ε -neighborhood for each point during a single-range query. This can be done by introducing a reference point, as discussed below.

Suppose $z_{p_i,1}$ is the projection of $x_{p_i} \in D$ in the first principal component ϕ_1 obtained by Algorithm 2, $i = 1, \dots, n$, and $z_{p_1,1}, z_{p_2,1}, \dots, z_{p_n,1}$ are arranged in decreasing order. If $|z_{p_i,1} - z_{p_j,1}| > \varepsilon$ for some positive integers i, j with $j \leq i \leq n$, then we have $|z_{p_j,1} - z_{p_k,1}| > \varepsilon$ for any integer k with $i \leq k \leq n$ and so, by Theorem 1 (i), $x_{p_k} \notin N_\varepsilon(x_{p_j})$ for $i \leq k \leq n$. As a result, we do not need to consider the point x_{p_k} for $j \leq k \leq n$ when we do the range query for x_{p_j} , that is, when we search for the ε -neighborhood of x_{p_j} . Hence, the number of accesses in range query is reduced. Further, The calculation of the distance between x_{p_k} and x_{p_j} can be pruned in batch for all integers k 's with $j \leq k \leq n$.

In the above process, only the projection on the first principal component ϕ_1 is considered for each data point. Unfortunately, this may lead to a wrong conclusion that the distance of the projections z_i, z_j on the first principal component ϕ_1 of certain data points $x_i, x_j \in D$ is smaller than ε , but the distance between the points x_i, x_j may actually be quite large, especially when the dimension d of the data points is high. A natural way to address this issue is to consider projections on the first n_a principal components $\phi_1, \phi_2, \dots, \phi_{n_a}$ for the data points with the integer $n_a \geq 1$, as illustrated in Figure 1. However, it is not easy to extend the process discussed in the preceding paragraph from the projections on the first principal component to those on the first several principal components. We will do this by introducing a reference point.

Note that Figure 1 (a) presents the projections on the first two principal components of the data points represented by the blue points, whilst Figure 1 (b) shows the projections on the first principal components of these data points. From Figure 1 it is clear that the projections on the first two principal components of the data points are very well separated (see Figure 1 (a)), but the projections on the first principal component of some data points are very close or even almost coincide (see Figure 1(b)).

For an integer $n_a \geq 1$ let $q = \sum_{j=1}^{n_a} q_j \phi_j$ be a reference point. Hereafter, for convenience, we call such q an n_a -dimensional point and write $q = (q_1, \dots, q_{n_a})$. Set

$$\hat{z}_i = z_i^0 + z_i^1, \quad (7)$$

where $z_i^0 = \sum_{k=1}^{n_a} z_{i,k} \phi_k$ and $z_i^1 = \sum_{k=n_a+1}^{h_1} z_{i,k} \phi_k$. Then

$$\|\hat{z}_i - \hat{z}_j\|^2 = \|z_i^0 - z_j^0\|^2 + \|z_i^1 - z_j^1\|^2 \quad (8)$$

with

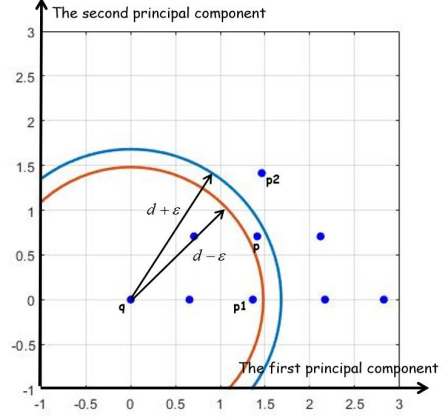
$$\begin{aligned} \|z_i^0 - z_j^0\| &= \|z_i^0 - q + q - z_j^0\| \\ &\geq \left| \|z_i^0 - q\| - \|z_j^0 - q\| \right| = |d_i - d_j|, \end{aligned} \quad (9)$$

where

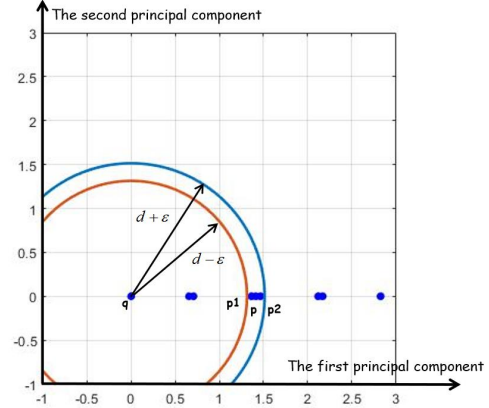
$$d_i := \|q - z_i^0\|, \quad i = 1, \dots, n. \quad (10)$$

Rearrange d_1, \dots, d_n in decreasing order as $d_{p_1}, d_{p_2}, \dots, d_{p_n}$ and set $d = [d_{p_1}, d_{p_2}, \dots, d_{p_n}]$. Then we have the following result which can be used to prune unnecessary distance calculations for a batch of points at once.

Theorem 2. For any two different points $x_{p_m}, x_{p_k} \in D$ with $0 < m < k \leq n$, if $|d_{p_m} - d_{p_k}| > \varepsilon$ then $\{x_{p_l}, n \geq l \geq k\} \not\subset N_\varepsilon(x_{p_m})$ and $\{x_{p_l}, 0 < l \leq m\} \not\subset N_\varepsilon(x_{p_k})$.



(a)



(b)

Fig. 1. An example for the phenomenon of the "overcrowding effect" and the choice of reference points

Proof. By (4), (7), (8), (9) and (10) it follows that for $n \geq l \geq k$ we have

$$\begin{aligned} \|x_{p_l} - x_{p_m}\| &\geq \|\hat{z}_{p_l} - \hat{z}_{p_m}\| \geq \|z_{p_l}^0 - z_{p_m}^0\| \\ &\geq |d_{p_l} - d_{p_m}| \geq |d_{p_k} - d_{p_m}| > \varepsilon. \end{aligned}$$

This implies that $x_{p_l} \notin N_\varepsilon(x_{p_m})$. The case $0 < l \leq m$ can be proved similarly. \square

Figure 1 (a) illustrates the significance of choosing a two-dimensional reference point in pruning unnecessary distance calculations. Suppose we want to search for the ε -neighborhood of the point whose projection on the first two principal components ϕ_1, ϕ_2 is p . The annular region associated with p is given by

$$R_p = \{z = \sum_{j=1}^2 z_j \phi_j : d - \varepsilon \leq \|z - q\| \leq d + \varepsilon\},$$

where $d = \|p - q\|$ and q is a two-dimensional reference point defined as $q = \sum_{j=1}^2 q_j \phi_j$. By Theorem 2 there is no need to access all the points whose projections on ϕ_1, ϕ_2 are

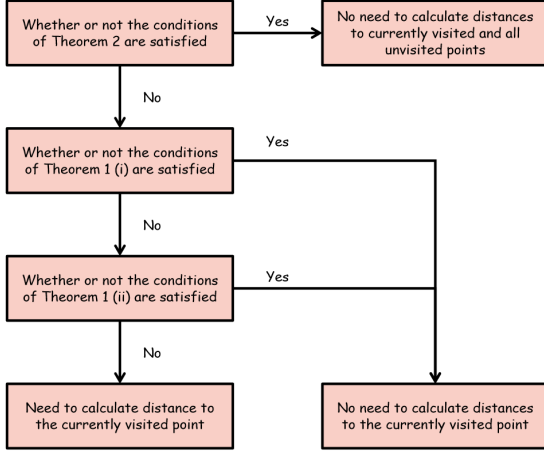


Fig. 2. The main idea of the neighborhood finding process.

outside of the annular region R_p in the process of finding an ε -neighborhood of p .

Based on Theorems 1 and 2, we propose a Fast PCA Pruning (FPCAP) algorithm to accelerate the range query for $x_{p_m} \in D$ in neighborhood finding. The main idea of the FPCAP algorithm is shown in Figure 2, and the detailed algorithm is given in Algorithm 3. Algorithm 3 can be roughly divided into four stages. Stage I excludes all the points on one side of $x_{p_{m+t}}$, that is, Stage I reduces the redundant distance calculations in batches. Stages II and III exclude the point at which the current iteration is reached if the condition in Step 4 or Step 6 in Algorithm 3 holds. In Stage IV, we have to calculate the distance between x_{p_m} and $x_{p_{m+t}}$ to see if $x_{p_{m+t}}$ is in the neighborhood of x_{p_m} :

$$d_{p_m, p_{m+t}} = \|x_{p_m} - x_{p_{m+t}}\|.$$

When we do range query for x_{p_k} , the parameter $\text{step} = 1$ or -1 in Algorithm 3 means finding neighbors of x_{p_k} from the set $\{x_{p_j} | k < j \leq n\}$ or $\{x_{p_j} | 0 < j < k\}$.

The reference point q in Algorithm 3 needs to be given in advance, and its choice is essential for the effectiveness of the algorithm. In this paper, the n_a -dimensional reference point q ($n_a \geq 1$) is chosen as

$$q = (Z_{\min, n_a}, \dots, Z_{\min, n_a}) = Z_{\min, n_a} \sum_{j=1}^{n_a} \phi_j, \quad (11)$$

where

$$Z_{\min, n_a} := \min\{z_{i,j} : 1 \leq i \leq n, 1 \leq j \leq n_a\}$$

and $Z = (z_{i,j})_{n \times h}$ is the projection of the data obtained by Algorithm 2, that is, $x_i = \sum_{j=1}^h z_{i,j} \phi_j$ for $x_i \in D$ with $z_{i,j} = \langle x_i, \phi_j \rangle$, $i = 1, \dots, n$, $j = 1, \dots, h$ (see the beginning of this section). Thus

$$\begin{aligned} d_i &= \|q - z_i^0\| \\ &= \left(\sum_{j=1}^{n_a} |z_{i,j} - Z_{\min, n_a}|^2 \right)^{1/2}, \quad i = 1, \dots, n. \end{aligned} \quad (12)$$

Algorithm 3 FPCAP

Input: row data matrix $X = [x_1, x_2, \dots, x_n]^T$ of size $n \times h$, projection data matrix $Z = [z_1, z_2, \dots, z_n]^T$ of size $n \times h$, candidate point x_{p_m} , reference point q , ε , step, h_1 , $t = 0$, $h' = 1$, Diff = 0.

Output: ε -neighborhood $N_\varepsilon(x_{p_m})$ of x_{p_m} .

- 1: Calculate $d_i = \|q - z_i^0\|$ for $i = 1, \dots, n$, and rearrange them in decreasing order as $d_{p_1}, d_{p_2}, \dots, d_{p_n}$.
- 2: $t = t + \text{step}$
- 3: If $m + t > n$, stop.
- 4: Stage I: Calculate

$$d = |d_{p_m} - d_{p_{m+t}}|.$$

If $d > \varepsilon$, stop.

- 5: Stage II: Calculate

$$\text{Diff} := \text{Diff} + \|z_{p_m, h'} - z_{p_{m-t}, h'}\|^2.$$

If $\text{Diff} > \varepsilon^2$, go to Step 2.

- 6: Update $h' = h' + 1$. If $h' \leq h_1$, go back to Step 5.
- 7: Stage III: Calculate

$$\begin{aligned} \|\tilde{z}_{p_m}\|_2 &= (\|x_{p_m}\|^2 - \|\hat{z}_{p_m}\|^2)^{1/2}, \\ \|\tilde{z}_{p_{m+t}}\| &= (\|x_{p_{m+t}}\|^2 - \|\hat{z}_{p_{m+t}}\|^2)^{1/2}. \end{aligned}$$

If $\text{Diff} + (\|\tilde{z}_{p_m}\| - \|\tilde{z}_{p_{m+t}}\|)^2 > \varepsilon^2$, go to Step 2.

- 8: Stage IV: Calculate

$$d_{p_m, p_{m+t}} = \|x_{p_m} - x_{p_{m+t}}\|.$$

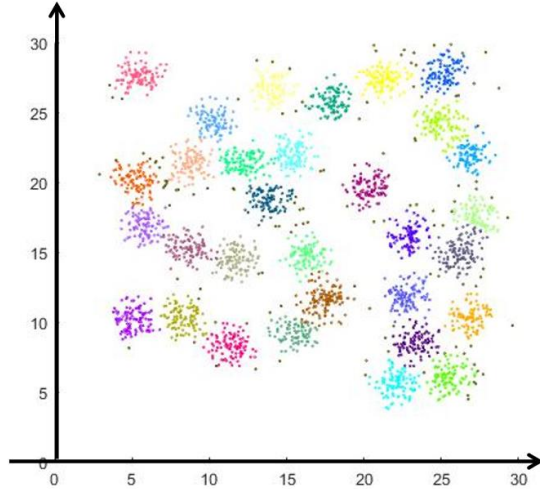
If $d_{p_m, p_{m+t}} \leq \varepsilon$, Update

$$N_\varepsilon(x_{p_m}) = N_\varepsilon(x_{p_m}) \cup \{x_{p_{m+t}}\}$$

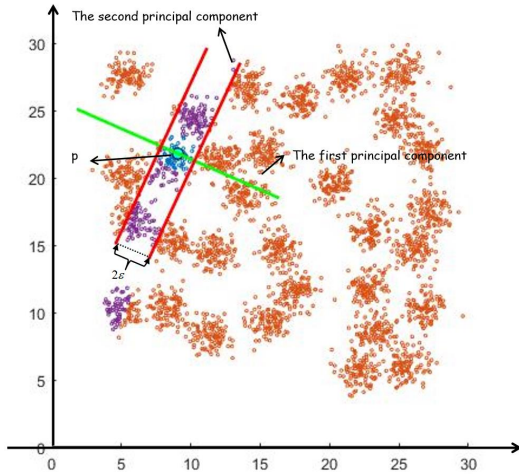
and go to Step 2.

Note that the special case when $n_a = 1$ is considered in [21] in a different context where the Fast-PCA technique [22] was applied to accelerate the global k -means algorithm proposed in [23]. In this case the one-dimensional reference point $q = \min_{1 \leq i \leq n} z_{i,1}$, where $z_{i,1}$ is the projection value of x_i along the first principal component ϕ_1 , that is, $z_{i,1} = \langle x_i, \phi_1 \rangle$, so $d_i = |z_{i,1} - q|$, $i = 1, \dots, n$.

Figure 3 illustrates the pruning process in Stages I and II in Algorithm 3 on the D31 data set which is a two-dimensional synthetic data sets with 3100 cardinalities and 31 clusters. Figure 3 (a) shows the clustering results of the DBSCAN algorithm with $\varepsilon = 1.32$ and MinPts = 68. In Figure 3 (b), the green and red lines represent the directions of the first and second principal components, respectively. The distances between the big green point p and the two red lines both are ε . When we search for the ε -neighborhood for p , the orange points and the purple points represent the data points pruned in Stages I and II in Algorithm 3, while the blue points are the ones whose distances to p must be calculated. The results show that there are only a small number of points whose distances to p really need to be calculated. In other words, Algorithm 3 can prune unnecessary distance calculations effectively when finding neighbors and estimating densities.



(a)



(b)

Fig. 3. Illustration of pruning process in Stages I and II in Algorithm 3

B. An improved DBSCAN (IDBSCAN) algorithm

The proposed FPCAP algorithm can be used together with a density-based clustering algorithm to get an improved density-based clustering algorithm. Figure 4 shows the framework of the proposed FPCAP algorithm combined with a density-based clustering algorithm which consists of the initialization stage (Stage I) and the clustering stage (Stage II). The main part of the initialization stage is fast principal component analysis. A new representation of the h -dimensional raw data $D = \{x_1, x_2, \dots, x_n\}$ can be obtained from this stage with $Z = (z_{p_i, j})_{n \times h}$ being the projection of data obtained by Algorithm 2. The clustering stage is the combination of the density-based clustering algorithm and the FPCAP algorithm. The final clustering results are obtained after this stage.

As an example of the above framework, in this subsection, the FPCAP algorithm is applied in the neighborhood-finding process of the DBSCAN algorithm to get an improved

DBSCAN (IDBSCAN) algorithm. The detailed IDBSCAN algorithm is given in Algorithm 4.

Algorithm 4 IDBSCAN

Input: row data matrix $X = [x_1, x_2, \dots, x_n]^T$ of size $n \times h$, ε , p

Output: the clustering result

- 1: Get the projection data matrix $Z = [z_1, z_2, \dots, z_n]^T$ of size $n \times h$ by Algorithm 2
 - 2: Choose the reference point q as in (11)
 - 3: Run Algorithm 1 (DBSCAN) with Algorithm 3 (FPCAP) used in the neighborhood-finding process
 - 4: Return the clustering result
-

1) *Correctness analysis:* In view of the indeterminacy in DBSCAN-like methods, border points may belong to different clusters in the case when the order of the data points appeared in DBSCAN and IDBSCAN is different. However, if the order of the data points appeared in DBSCAN and IDBSCAN is assumed to be the same, then IDBSCAN and DBSCAN produce the same result. On the other hand, by Theorems 1 and 2 (see also Figure 2) the conditions in Stages I, II and III in Algorithm 3 are only used to justify if $x_{p_{m+t}} \notin N_\varepsilon(x_{p_m})$, and if the conditions in Stages I, II and III in Algorithm 3 are not satisfied then we need to calculate the distance between the original points $x_{p_{m+t}}$ and x_{p_m} to see if $x_{p_{m+t}} \in N_\varepsilon(x_{p_m})$ (see Stage IV in Algorithm 3). Hence, IDBSCAN and DBSCAN obtain the same ε -neighborhood result. Since the process of IDBSCAN is the same as that of DBSCAN except for the different methods in finding ε -neighborhoods, IDBSCAN improves the efficiency of DBSCAN without losing correctness under the assumption that the order of the data points appeared in DBSCAN and IDBSCAN is the same. Even without the above assumption, DBSCAN and IDBSCAN still produce the same clustering result if we only consider the clustering result of core points.

2) *Complexity analysis:* We focus on the time complexity analysis about the distance calculation which dominates the runtime of the range query in FPCAP (Algorithm 3). Denote by n_1 the total number of pruning in Stage I of Algorithm 3, and denote by n_2 the total number of pruning for range query in Stages II and III of Algorithm 3. Thus, on searching for the ε -neighborhood for x_{p_j} in Algorithm 3, if the condition $|d_{p_j} - d_{p_k}| > \varepsilon$ is satisfied for $j < k \leq n$ then n_1 is increased by $n - (k - 1)$, and if the conditions in Theorem 1 are satisfied for x_{p_j} and x_{p_k} then n_2 is increased by 1. Define n_0 to be the average number of distance computations in Stage IV. Then

$$n_0 := (n - 1) - \frac{n_1}{n} - \frac{n_2}{n}. \quad (13)$$

The complexity of calculation of (10) and (6) is $O(nn_a)$ and $O(nh)$, respectively. The complexity of Stages II and IV is $O(n(n - n_1/n)h_1)$ and $O(n(n - n_1/n - n_2/n)(h - h_1))$, respectively. As a result, the whole time complexity of FPCAP (Algorithm 3) is $O(nn_a + n(n - n_1/n)h_1 + n(n - n_1/n - n_2/n)(h - h_1) + nh)$. In the case when $n - n_1/n = O(1)$, the complexity is $O(nh)$, which is a very good improvement. Take the experiments conducted on

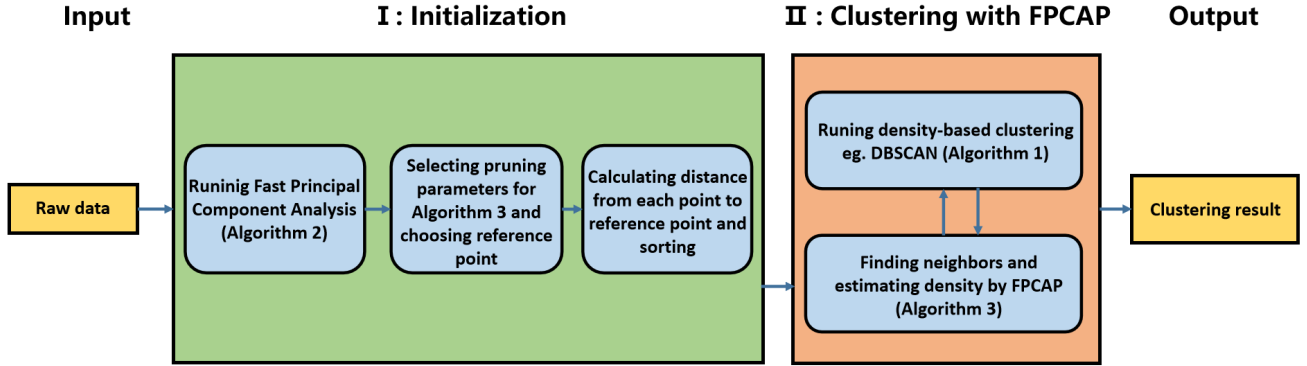


Fig. 4. The framework of the proposed FPCAP algorithm combined with a density-based clustering algorithm

the subset of Reactionnetwork data set ($n=20000$) in Section V as example, when $n_a = 1$ and $\varepsilon = 1000, 10000, 20000$ and 30000 , $n_1/n = 19615, 17125, 14706$ and 12387 and $n_0 = 110, 147, 452$ and 1162 . When ε is small, the value of $n - n_1/n \ll n$ and $n_0 \ll n$. In addition, when $p = 0.8$, $h_1 = h/7$ which is much smaller than h . Note that the FPCAP (Algorithm 3) includes the sorting process of the distance from the data points to the reference point, and its complexity is $O(n \log n)$, but its runtime is very short compared to the overall runtime of FPCAP (Algorithm 3).

IV. EXPERIMENTAL RESULTS

A. Data sets

We now conduct several experiments on four real-world data sets and three synthetic data sets to illustrate the efficiency of the FPCAP and the IDBSCAN algorithms. Clickstream is a 12-dimensional real-world data set with 165474 cardinalities which are composed of information on clickstream from online stores offering clothing for pregnant women. Household is a 7-dimensional real-world data set with 2049280 cardinalities including all attributes except the temporal columns data and time. Mocap is a 36-dimensional real-world data set with 78095 cardinalities, which has 5 types of hand postures from 12 users. ReactionNetwork is a KEGG Metabolic Reaction Network (Undirected) Data set of 65554 data points of 28 dimensions. Dim-set consists of three synthetic datasets, Dim6, Dim10, Dim15, with Gaussian clusters and 4051, 6751 and 10126 cardinalities, respectively. The above real-world data sets and synthetic data sets can be downloaded from the UCI Machine Learning repository¹ and clustering datasets website², respectively. Duplicated data points and points with missing coordinates are deleted. Each attribute of the data is normalized to $[0, 100000]$.

¹<http://archive.ics.uci.edu/ml/>

²<http://cs.joensuu.fi/sipu/datasets/>

B. Algorithms

The following algorithms are used in the experiments:

- FPCAP₁: Fast-PCA pruning initialized with the one-dimensional reference point q given by (11) with $n_a = 1$,
- FPCAP₂: Fast-PCA pruning initialized with the two-dimensional reference point q given by (11) with $n_a = 2$,
- KD tree: KD tree indexing technique on row data,
- KD tree with PCA: KD tree indexing technique on projected data obtained with Fast-PCA (Algorithm 2).

All the experiments are conducted on a single PC with Intel Core 2.9GHz i7 CPU (16 Cores) and 32G RAM.

C. Experimental results

1) *Experiment 1: Effect of the choice of the reference point:* In the initialization process of FPCAP, the choice of the reference point is very important and needs to be determined first. Experiment 1 is conducted to compare the effect on the pruning result of the dimensionality n_a of the reference point q . The value of n_1 appearing in the expression (13), which is the total number of pruning in Stage I of Algorithm 3, determines the total number of accesses during range query, that is, the total number of distance calculations in Stage II in Algorithm 3 which dominates the runtime of Algorithm 4. Therefore, Experiment 1 evaluates the initialization method in terms of the dimensionality n_a of the reference point q , based on n_1 . Figure 5 presents the experimental results on the number of pruning calculations in Stage I of Algorithm 3 against the dimensionality n_a of the reference point q for different neighborhood parameter ε on the three synthetic datasets, Dim6, Dim10, Dim15, and the subsets of the four real-world data sets, Clickstream, Household, Mocap and Reactionnetwork, with each subset containing 20000 data points. From Figure 5 we have the following observations: 1) Initializing with a two-dimensional reference point (i.e., $n_a = 2$) outperforms the other cases with $n_a \neq 2$ on most of the data sets used in the experiments such as Dim6, Dim10, Dim15, Clickstream and Household for different choices of ε ; this

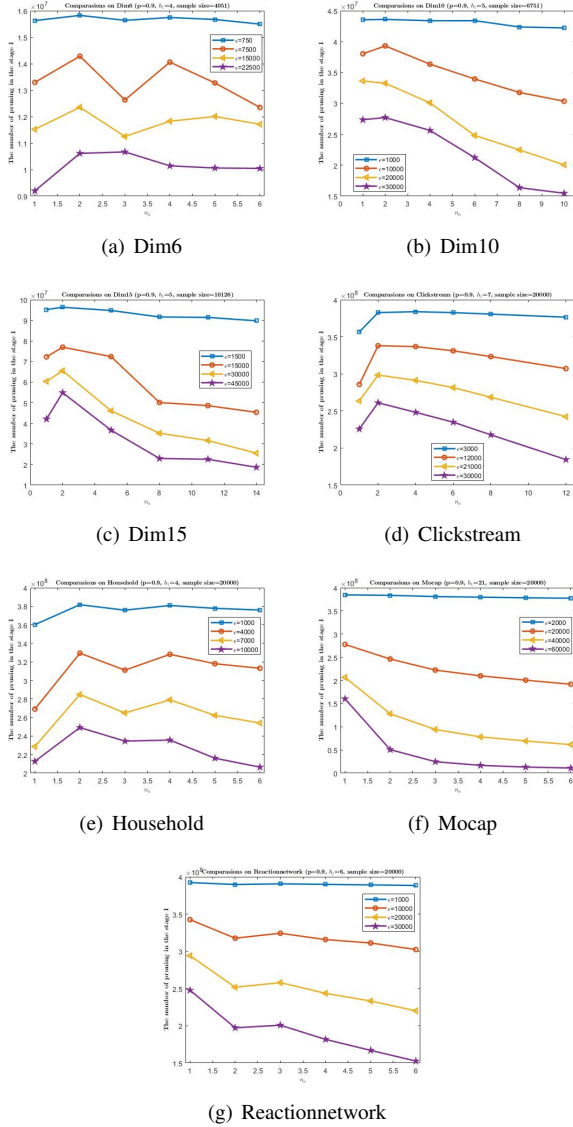


Fig. 5. The number of pruning against the dimensionality n_a of the reference point q on seven data sets

means that the initialization with $n_a = 2$ can effectively reduce the number of accesses during range query; 2) Initializing with a one-dimensional reference point (i.e., $n_a = 1$) outperforms the other cases with $n_a > 1$ on Mocap and Reactionnetwork for different choice of ε . Based on the above observations, we use the cases $n_a = 1, 2$ to initialize FPCAP (i.e., FPCAP₁ and FPCAP₂) in the remaining experiments.

2) *Experiment 2: Effect of the neighborhood radius ε in range query:* Experiment 2 compares the four algorithms, FPCAP₁, FPCAP₂, KD tree and KD tree with PCA, on the same seven data sets as used in Experiment 1 for different ε , in terms of their runtime and n_0 (i.e., the total number of distance calculations). Note that the runtime of the four algorithms was recorded as the average over 10 duplicate tests to reduce randomness. Figure 6 presents the runtime of the four algorithms against ε . The results show that FPCAP₁ and FPCAP₂ outperforms both KD tree and KD tree with PCA greatly on the three synthetic data sets and three real-

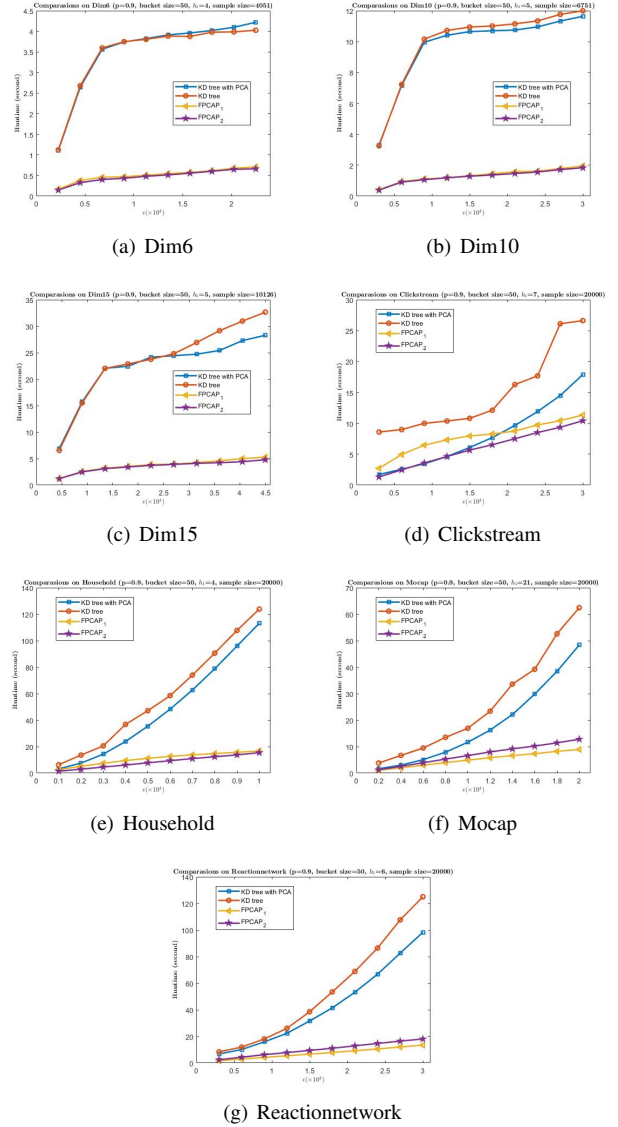


Fig. 6. The runtime of the four algorithms on the seven data sets with different ε

world data sets, Household, Mocap and Reactionnetwork, and FPCAP₁, FPCAP₂ and KD tree with PCA outperforms KD tree on Clickstream with FPCAP₂ having the best performance among the four algorithms, KD tree with PCA performing better than FPCAP₁ when $\varepsilon < 2$ and FPCAP₁ having a better performance than KD tree with PCA when $\varepsilon > 2$. Further, it is seen from Figure 6 that the performance of FPCAP₁ and FPCAP₂ is similar on the seven data sets with FPCAP₂ performing slightly better than FPCAP₁ on the three synthetic data sets and two real-world data sets, Clickstream and Household, and FPCAP₁ performing slightly better than FPCAP₂ on Mocap and Reactionnetwork. Furthermore, Figure 6 shows that the runtime of KD tree and KD tree with PCA increases much faster than FPCAP₁ and FPCAP₂ with ε increasing. Figure 7 presents the value of n_0 (i.e., the total number of distance calculations) of the pruning algorithms, KD tree, KD tree with PCA and FPCAP, against ε . The results in Figure 7 illustrate that, compared to the KD indexing

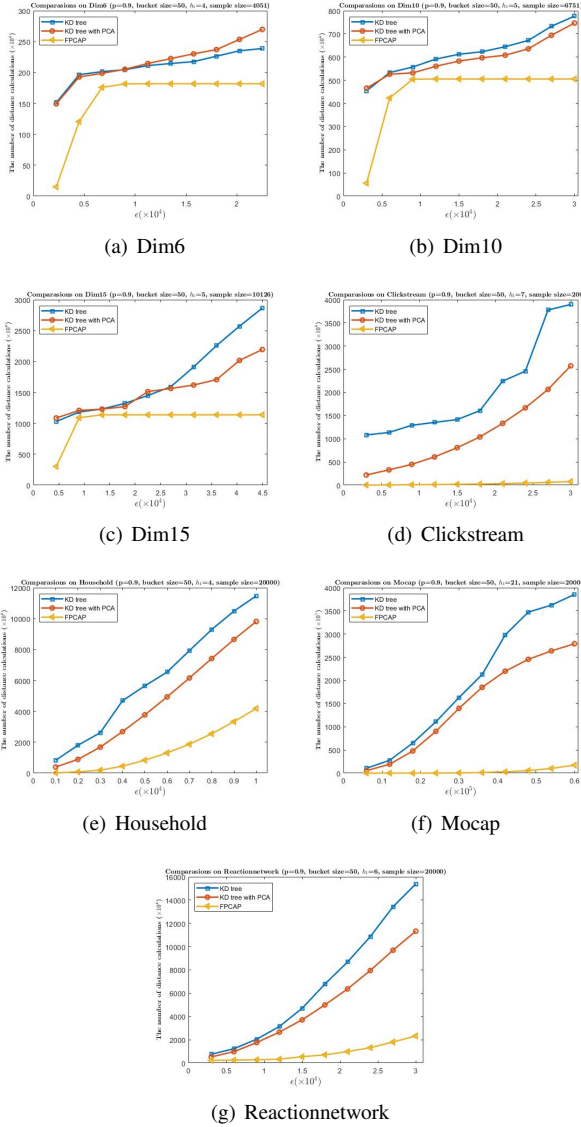


Fig. 7. The number of distance calculations on the seven data sets with different ε

technique, FPCAP reduces more distance calculations.

3) *Experiment 3: Effect of the cardinality (data sample size) on the runtime*: Experiment 3 was conducted to compare the runtime of the four algorithms, FPCAP₁, FPCAP₂, KD tree and KD tree with PCA, on the subsets of the four real-world data sets, Clickstream, Household, Mocap and Reactionnetwork, for different cardinality (or data sample size).

Figure 8 presents the runtime of FPCAP₁, FPCAP₂, KD tree and KD tree with PCA against the data sample size n on the subsets of the four real-world data sets. The results in Figure 8 show that FPCAP (FPCAP₁ and FPCAP₂) significantly outperforms the KD tree indexing techniques (KD tree and KD tree with PCA) as n increases. It is further seen from Figure 8 that the runtime of KD tree and KD tree with PCA increases much faster than that of FPCAP₁ and FPCAP₂ with n increasing.

4) *Experiment 4: Performance of FPCAP in combination with DBSCAN*: In this experiment we examine the perfor-

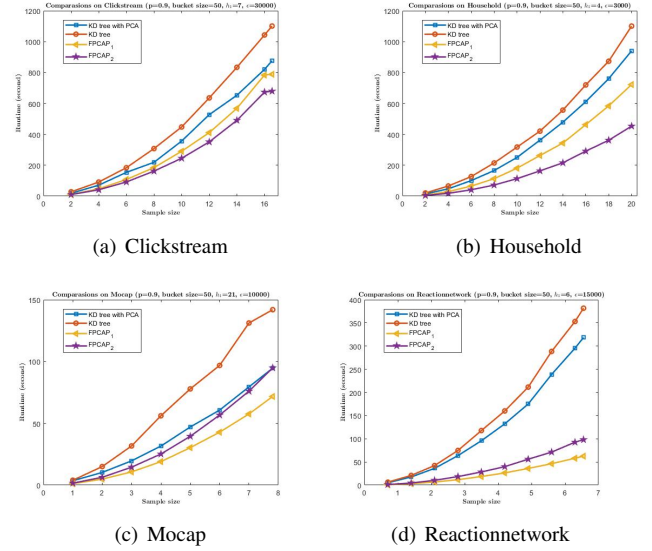


Fig. 8. The runtime of the four algorithms against the cardinality (or data sample size) on the four real-world data sets. The unit of the sample size is ten thousand.

mance of the Fast-PCA pruning algorithm, FPCAP, in combination with DBSCAN. This we do by comparing with the naive way of neighbourhood finding and the KD tree indexing technique in combination with the DBSCAN algorithm. The five comparing algorithms are as follows:

- DBSCAN: The original DBSCAN algorithm (Algorithm 1) without pruning in the neighbourhood finding process;
- DBSCAN₁: DBSCAN (Algorithm 1) with the KD tree indexing technique on the projected data obtained through Fast-PCA (Algorithm 2);
- DBSCAN₂: DBSCAN (Algorithm 1) with KD tree indexing technique on row data;
- IDBSCAN₁: IDBSCAN (Algorithm 4) with $n_a = 1$;
- IDBSCAN₂: IDBSCAN (Algorithm 4) with $n_a = 2$.

We first compare the runtime of the five comparing algorithms for different ε , Minpts and p . Table I shows their runtime against p . From Table I it is seen that (1) IDBSCAN has the best performance on all seven data sets in terms of runtime; (2) the KD tree indexing technique combined with Fast-PCA (DBSCAN₁) outperforms the original KD tree indexing technique (DBSCAN₂) on all the four real-world data sets (except for the three synthetic datasets, Dim6, Dim10, Dim15, on which the performance of the two algorithms are similar); (3) for large ε , DBSCAN with the KD tree indexing techniques (DBSCAN₁ and DBSCAN₂) need a much longer runtime than the original DBSCAN algorithm does on the three synthetic data sets, Dim6, Dim10 and Dim15; (4) the parameter p varies from 0.7 to 0.99, but the runtime of IDBSCAN₁ and IDBSCAN₂ does not change largely, meaning that the runtime of IDBSCAN₁ and IDBSCAN₂ is not sensitive to the choice of the parameter p . In addition, Figure 9, which presents the total runtime of performing Fast-PCA and KD tree construction, illustrates that the time used in initialization, that is, the runtime of Fast-PCA is negligible compared with that of IDBSCAN and that the runtime of fast-

PCA is much smaller than that of the construction of the KD tree.

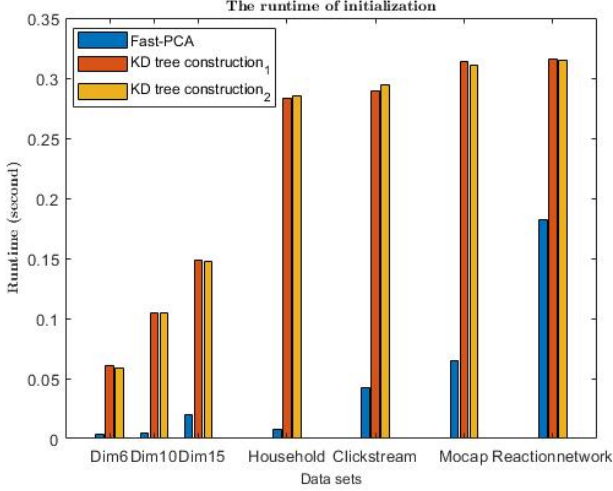


Fig. 9. The total runtime of performing Fast-PCA and KD tree construction, where KD tree construction₁ stands for the construction of KD tree on row data and KD tree construction₂ represents the construction of KD tree on projected data obtained by Fast-PCA (Algorithm 2).

D. Comprehensive analysis: Range query in high dimensions

Theorem 3. Suppose the sample points $\{x_1, \dots, x_n\}$ are uniformly distributed in a d -dimensional hypercube S with side length r . Denote by $R_{d,e}(x)$ the fraction of the sample points captured by a d -dimensional sphere of radius r_0 and centered at $x \in S$, where $e = r_0/r$. If $0 \leq e \leq 1/2$ then it follows that for any $x \in S$,

$$L_{d,e} \leq R_{d,e}(x) \leq U_{d,e},$$

where $L_{d,e} = V_d(1)e^d 2^{-d}$, $U_{d,e} = V_d(1)e^d$ and $V_d(r) = \pi^{d/2} r^d / \Gamma((d/2)+1)$ is the volume of a sphere of radius r with the Gamma function $\Gamma(t)$ for $t > 0$ satisfying that $\Gamma(t+1) = t\Gamma(t)$ and $\Gamma(1/2) = \sqrt{\pi}$.

Proof. Denote by $W_d(r)$ the volume of the hypercube with side length r . In the case when the sphere of radius r_0 and centered at $x \in S$ is inside of the hypercube with side length r without intersection, as seen in Figure 10 (a), we have $R_{d,e}(x) = V_d(r_0)/W_d(r) = V_d(1)e^d$ which is independent of $x \in S$ and thus is an upper bound of $R_{d,e}(x)$ for all $x \in S$. In the case when the center $x \in S$ of the sphere locates at one of the vertices of the hypercube, as seen in Figure 10 (b), we have $R_{d,e}(x) = V_d(r_0)/[W_d(r)2^d] = V_d(1)e^d 2^{-d}$ which is a lower bound of $R_{d,e}(x)$. \square

Figure 11 presents the relationship between the radius of the sphere and the upper bound $U_{d,e}$ of $R_{d,e}(x)$ given in Theorem 3. The results illustrate the sparsity of high-dimensional data in the sense that for high-dimensional data which are uniformly distributed in a d -dimensional hypercube S of side length r , the number of the data points contained in a sphere of radius r_0 and centered at $x \in S$ is getting much smaller with d increasing when $r_0/r \leq 1/2$. For example, for sample

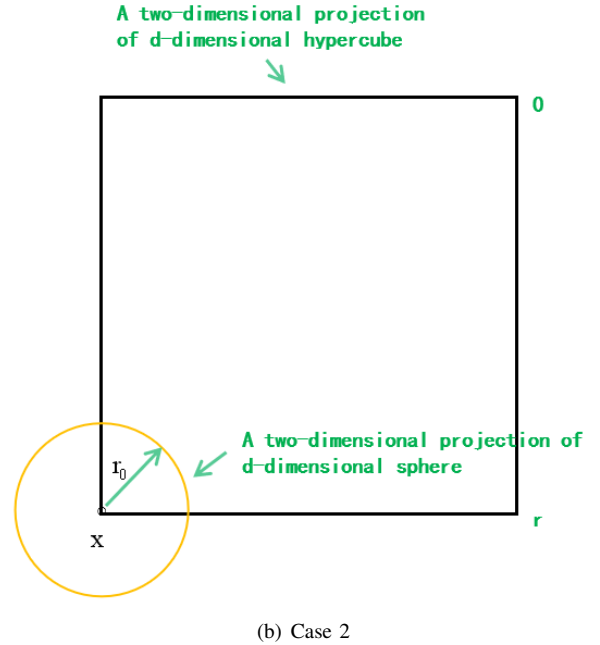
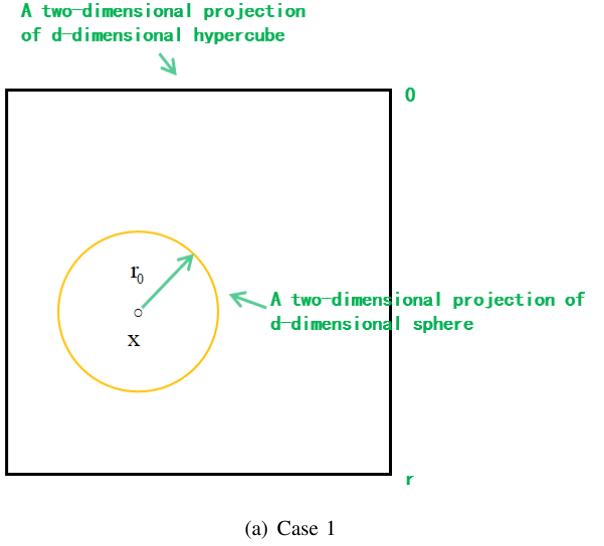


Fig. 10. Range query in high dimensions

points uniformly distributed in a d -dimensional hypercube S of side length r , if $d > 20$ then the sphere of radius $r/2$ and centered at $x \in S$ only contains 2.46×10^{-8} percent of the total number of sample points. Consider the process of the DBSCAN algorithm. Due to the sparsity of high-dimensional data, the search radius of range query increases with the dimension d . For the KD tree indexing technique, the larger the search radius is, the more sample points need to be accessed in the process of range query, thus reducing the efficiency of range query. Therefore, for the range query method combined with the KD tree indexing technique, when the search radius is bigger than $r/2$, at least 50 percent of the sample points need to be accessed in each range query.

Data sets	[MinPts, ϵ]	DBSCAN	DBSCAN ₁	DBSCAN ₂	$p(h_1)$	IDBSCAN ₁	IDBSCAN ₂
Clickstream	[10, 15000]	22.09	6.45	11.33	80% (6)	7.77	5.83
					90% (7)	8.13	5.97
					99% (9)	7.82	5.96
	[20, 30000]	22.50	18.33	27.31	80% (6)	11.72	11.18
					90% (7)	11.74	11.13
					99% (9)	11.67	11.11
Household	[5, 1000]	19.88	3.47	6.66	80% (2)	2.73	1.59
					90% (4)	2.76	1.61
					99% (6)	2.80	1.63
	[10, 3000]	19.98	14.45	20.60	80% (2)	7.59	4.72
					90% (4)	7.51	4.89
					99% (6)	7.48	4.89
Dim6	[3, 1500]	0.82	0.78	0.80	70% (3)	0.14	0.13
					90% (4)	0.13	0.13
					99% (6)	0.15	0.13
	[5, 5000]	1.04	3.15	3.15	70% (3)	0.48	0.43
					90% (4)	0.48	0.44
					99% (6)	0.47	0.41
Dim10	[3, 2000]	2.52	2.62	2.48	80% (3)	0.34	0.36
					90% (5)	0.34	0.35
					99% (8)	0.34	0.35
	[5, 6000]	2.89	7.43	7.45	80% (3)	0.98	0.97
					90% (5)	1.00	0.96
					99% (8)	1.01	0.97
Dim15	[3, 3000]	6.34	5.65	5.28	80% (4)	1.01	0.99
					90% (5)	1.03	0.96
					99% (8)	1.03	0.96
	[5, 9000]	7.14	16.34	16.11	80% (4)	2.77	2.63
					90% (5)	2.75	2.63
					99% (8)	2.69	2.61
Mocap	[5, 6000]	35.40	5.56	9.92	80% (15)	3.19	4.14
					90% (21)	3.30	4.07
					99% (31)	3.29	4.17
	[10, 14000]	35.85	23.18	34.92	80% (15)	7.03	9.21
					90% (21)	6.84	9.18
					99% (31)	6.98	9.22
Reactionnetwork	[3, 5000]	31.40	9.37	10.95	80% (4)	2.79	3.97
					90% (6)	2.80	3.93
					99% (12)	2.75	3.97
	[5, 10000]	30.94	18.55	21.08	80% (4)	4.92	7.30
					90% (6)	4.89	7.08
					99% (12)	4.96	7.12

TABLE I
RUNTIME (IN SECONDS) OF THE FIVE COMPARING ALGORITHMS ON FIVE BENCHMARK DATA SETS WITH DIFFERENT p .

V. CONCLUSION

In order to accelerate the process of range query in density-based methods which are one of the most popular clustering methods and have wide applications, we proposed a fast range query algorithm (called FPCAP), based on the fast principal component analysis which prunes unnecessary distance calculations in the range search process. By combining FPCAP with DBSCAN, we obtained an Improved DBSCAN (called IDBSCAN) algorithm. Experimental results on real-world and synthetic data sets demonstrate that both FPCAP and IDBSCAN improve the computational efficiency and outperform other compared methods. FPCAP can also be combined with other density-based clustering methods to improving their efficiency.

REFERENCES

- [1] P. Berkhin, "A survey of clustering data mining techniques," in *Grouping Multidimensional Data*. Springer, 2006, pp. 25–71.
- [2] A. Coates and A. Y. Ng, "The importance of encoding versus training with sparse coding and vector quantization," in *ICML*, 2011.
- [3] C. Boutsidis, A. Zouzias, M. W. Mahoney, and P. Drineas, "Randomized dimensionality reduction for k-means clustering," *IEEE Transactions on Information Theory*, vol. 61, no. 2, pp. 1045–1062, 2014.
- [4] G. D. Canas, T. Poggio, and L. Rosasco, "Learning manifolds with k-means and k-flats," *arXiv:1209.1121*, 2012.
- [5] M. Ester, H.-P. Kriegel, J. Sander, X. Xu et al., "A density-based algorithm for discovering clusters in large spatial databases with noise," in *KDD*, vol. 96, no. 34, 1996, pp. 226–231.
- [6] M. Ankerst, M. M. Breunig, H.-P. Kriegel, and J. Sander, "Optics: Ordering points to identify the clustering structure," *ACM Sigmod Record*, vol. 28, no. 2, pp. 49–60, 1999.
- [7] A. Rodriguez and A. Laio, "Clustering by fast search and find of density peaks," *Science*, vol. 344, no. 6191, pp. 1492–1496, 2014.

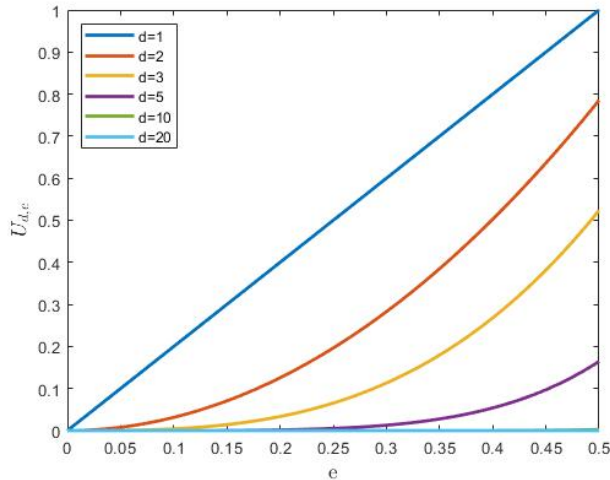


Fig. 11. The upper bound $U_{d,e}$ against e for dimension $d = 1, 2, 3, 5, 10, 20$, where $U_{d,e}$ and e are defined in Theorem 3. Note that when $e = 1/2$, $U_{d,e} = 1, 0.7854, 0.5236, 0.1645, 0.00249, 2.46 \times 10^{-8}$, corresponding to $d = 1, 2, 3, 5, 10, 20$, respectively.

- [8] Y. Cheng, "Mean shift, mode seeking, and clustering," *IEEE Transactions on Pattern Analysis and Machine Intelligence*, vol. 17, no. 8, pp. 790–799, 1995.
- [9] S. Anand, S. Mittal, O. Tuzel, and P. Meer, "Semi-supervised kernel mean shift clustering," *IEEE Transactions on Pattern Analysis and Machine Intelligence*, vol. 36, no. 6, pp. 1201–1215, 2013.
- [10] Y. Chen, L. Zhou, N. Bouguila, C. Wang, Y. Chen, and J. Du, "Block-dbscan: Fast clustering for large scale data," *Pattern Recognition*, vol. 109, p. 107624, 2021.
- [11] B. Borah and D. K. Bhattacharyya, "An improved sampling-based dbscan for large spatial databases," in *Proceedings of 2004 International Conference on Intelligent Sensing and Information Processing*. IEEE, 2004, pp. 92–96.
- [12] B. Liu, "A fast density-based clustering algorithm for large databases," in *Proceedings of 2006 International Conference on Machine Learning and Cybernetics*. IEEE, 2006, pp. 996–1000.
- [13] J. Jang and H. Jiang, "Dbscan++: Towards fast and scalable density clustering," in *International Conference on Machine Learning*. PMLR, 2019, pp. 3019–3029.
- [14] Y. Chen, S. Tang, N. Bouguila, C. Wang, J. Du, and H. Li, "A fast clustering algorithm based on pruning unnecessary distance computations in dbscan for high-dimensional data," *Pattern Recognition*, vol. 83, pp. 375–387, 2018.
- [15] S. Mahran and K. Mahar, "Using grid for accelerating density-based clustering," in *Proceedings of 8th IEEE International Conference on Computer and Information Technology*. IEEE, 2008, pp. 35–40.
- [16] A. Gunawan and M. de Berg, "A faster algorithm for dbscan," *Master Thesis*, 2013.
- [17] J. Gan and Y. Tao, "On the hardness and approximation of euclidean dbscan," *ACM Transactions on Database Systems (TODS)*, vol. 42, no. 3, pp. 1–45, 2017.
- [18] J. L. Bentley, D. F. Stanat, and E. H. Williams Jr, "The complexity of finding fixed-radius near neighbors," *Information Processing Letters*, vol. 6, no. 6, pp. 209–212, 1977.
- [19] A. Beygelzimer, S. Kakade, and J. Langford, "Cover trees for nearest neighbor," in *Proceedings of the 23rd international Conference on Machine learning*, 2006, pp. 97–104.
- [20] A. Guttman, "R-trees: A dynamic index structure for spatial searching," in *Proceedings of the 1984 ACM SIGMOD international conference on Management of data*, 1984, pp. 47–57.
- [21] J. Z. Lai and T.-J. Huang, "Fast global k-means clustering using cluster membership and inequality," *Pattern Recognition*, vol. 43, no. 5, pp. 1954–1963, 2010.
- [22] A. Sharma and K. K. Paliwal, "Fast principal component analysis using fixed-point algorithm," *Pattern Recognition Letters*, vol. 28, no. 10, pp. 1151–1155, 2007.
- [23] A. Likas, N. Vlassis, and J. J. Verbeek, "The global k-means clustering algorithm," *Pattern Recognition*, vol. 36, no. 2, pp. 451–461, 2003.
- [24] A. Hyvärinen and E. Oja, "A fast fixed-point algorithm for independent component analysis," *Neural computation*, vol. 9, no. 7, pp. 1483–1492, 1997.
- [25] J. L. Bentley, "Multidimensional binary search trees used for associative searching," *Communications of the ACM*, vol. 18, no. 9, pp. 509–517, 1975.



Difei Cheng received BSc degree in mathematics and applied mathematics from Shandong University, Jinan, China, in 2017. He is currently pursuing his PhD degree in machine learning and pattern recognition with Institute of Applied Mathematics, Academy of Mathematics and Systems Science, Chinese Academy of Sciences, Beijing, China.

His current research interests include clustering, unsupervised feature learning, manifold learning, metric learning and deep learning.



Ruihang Xu received BSc degree in mathematics and statistics from Xidian University, Xi'an, China, in 2018. He is currently pursuing his PhD degree in machine learning with Institute of Applied Mathematics, Academy of Mathematics and Systems Science, Chinese Academy of Sciences, Beijing, China. His current research interests include deep learning and image processing.



Bo Zhang (M'10) received BSc degree in mathematics from Shandong University, Jinan, China, MSc degree in mathematics from Xi'an Jiaotong University, Xi'an, China, and PhD degree in applied mathematics from the University of Strathclyde, Glasgow, UK, in 1983, 1985, and 1992, respectively.

After being a postdoc at Keele University, UK and a Research Fellow at Brunel University, UK, from 1992 to 1997, he joined Coventry University, Coventry, UK, in 1997, as a Senior Lecturer, where he was promoted to Reader in Applied Mathematics

in 2000 and to Professor of Applied Mathematics in 2003. He is currently a Professor with Institute of Applied Mathematics, Academy of Mathematics and Systems Science, Chinese Academy of Sciences, Beijing, China. His current research interests include direct and inverse scattering problems, radar and sonar imaging, machine learning, and data mining. He is currently an Associate Editor of the IEEE TRANSACTION ON CYBERNETICS, and Applicable Analysis.



Ruinan Jin received the B.S.c. degree in Schiffsmotor from Wuhan University of Technology, China, in 2017. He is currently pursuing the M.Sc degree in machine learning and pattern recognition with Academy of Mathematics and Systems Science, Chinese Academy of Sciences, Beijing, China. His current research interests include stochastic optimization, unsupervised feature learning, deep learning theory, causal discovery.